# Hippocampal Interneuronal Dysfunction and Hyperexcitability in a Porcine Model of Concussion

Alexandra V. Ulyanova[1], Carlo Cottone[1], Christopher D. Adam[1], Nikhil Maheshwari[1], Michael R. Grovola[1], Oceane E. Fruchet[1], Jami Alamar[1], Paul F. Koch[1], Victoria E. Johnson[1], D. Kacy Cullen[1,2], and John A. Wolf[#1,2]

[1]Center for Brain Injury and Repair, Department of Neurosurgery, University of Pennsylvania, Philadelphia, PA

[2]Center for Neurotrauma, Neurodegeneration, and Restoration, Corporal Michael J. Crescenz Veterans Affairs Medical Center, Philadelphia, PA

[#]Corresponding author

Corresponding Author:

John A. Wolf, Ph.D.
Department of Neurosurgery
Perelman School of Medicine
172A Stemmler Hall
3450 Hamilton Walk
Philadelphia, PA, 19104
+1-(215)-746-4680
wolfjo@pennmedicine.upenn.edu

Running Title: Hippocampal excitability following concussion

Key Words: pig, inertial brain injury, concussion, mTBI, diffuse axonal injury, hippocampus, *in vivo* electrophysiology, silicon probes, interneurons, hyperexcitability.

**Abstract**

Cognitive impairment is a common symptom following mild traumatic brain injury (mTBI or concussion) and can persist for years in some individuals. While the underlying mechanisms driving these impairments remain unknown, structural changes in the hippocampus post-mTBI have been reported in human patients, as well as electrophysiological changes in rodents following impact models of TBI. In addition, slice preparations from a closed-head, rotational acceleration injury (RAI) in swine showed reduced axonal function and hippocampal circuitry disruption. However, electrophysiological changes in neurons and their subtypes have not been examined. Using *in vivo* electrophysiology techniques, we examined the laminar oscillatory field potentials and single unit activity in the intact hippocampal network at 7 days post-RAI in anesthetized minipigs. Concussion altered the electrophysiological properties of pyramidal cells and interneurons differently in area CA1. Specifically, while firing rate and burst occurrence of CA1 interneurons were significantly decreased post-mTBI, these parameters were unchanged in putative CA1 pyramidal cells. However, pyramidal CA1 cells in TBI animals were significantly less entrained to hippocampal gamma (40 - 80 Hz) oscillations. In addition, stimulation of the Schaffer collaterals revealed hyperexcitability in the laminar CA1 response post-mTBI. Finally, computational simulations suggest that the reported changes in interneuronal firing rate and action potentials may be due to alterations in voltage-gated sodium channels. These data demonstrate that a single concussion can lead to significant neuronal and circuit level changes in the hippocampus, and that the loss of pyramidal gamma entrainment and changes in interneuronal firing may be important contributors to cognitive dysfunction following mTBI.

## Introduction

Concussion, or mild TBI (mTBI), is a common form of brain injury, affecting approximately 1.3 million people every year in the US alone (Bazarian, McClung et al. 2005). Cognitive impairment is common following concussion and deficits in episodic memory, learning, and delayed recall have been described (Anita, Lori et al. 2008, Giza, Greco et al. 2018, de Freitas Cardoso, Faleiro et al. 2019). Importantly, a growing body of data suggests that neurocognitive dysfunction observed post-concussion can persist for years after initial insult in some people (Sterr, Herron et al. 2006, Røe, Sveen et al. 2009, King and Kirwilliam 2011, Rabinowitz, Li et al. 2015, Levin, Temkin et al. 2021). Given the important role of the hippocampus in learning and memory, it is a central region of interest in diseases affecting these cognitive processes (for review, see (Carr, Jadhav et al. 2011)). While the underlying mechanisms of cognitive dysfunction following mTBI remain largely unknown, structural changes in the human hippocampus up to 1-year post-concussion have been reported (Singh, Meier et al. 2014, Strain, Womack et al. 2015). Interestingly, recent reports also link concussion to hyperexcitability (Major, Rogers et al. 2015, King, Kirton et al. 2019) and an increased risk for post-traumatic epilepsy (Amit, Odeya et al. 2017).

Rodent studies of TBI have shown changes in neuronal firing and local hippocampal oscillations, potentially suggesting abnormalities in temporal coding, a crucial element of episodic memory formation and encoding (Broussard, Redell et al. 2020). Using a biomechanically relevant and gyrencephalic model of concussion in swine, we demonstrated a reduction in axonal function and injury-related compensatory mechanisms in the *ex vivo* hippocampus. Moreover, deafferentation of the temporal region via axonal pathology has been proposed as a driver of hyperexcitability observed in this model (Wolf, Johnson et al. 2017). Diffuse axonal injury, a predominant pathology observed in this preclinical model of concussion may disrupt the precise timing of hippocampal oscillations and associated neuronal activity, however these neurophysiological changes occurred in the apparent absence of intra-hippocampal neuronal or axonal degeneration (for review, see (Wolf and Koch 2016)). More

importantly, direct evidence that the hippocampal neuronal network, specific neuronal subtypes, or laminar hippocampal oscillations are affected by concussion in the intact animal has yet to be demonstrated.

After utilizing an established porcine model of closed-head, rotational acceleration to induce concussion, we then applied *in vivo* electrophysiology techniques to examine neuronal and oscillatory changes in the intact hippocampus at 7 days post-injury. Notably, hippocampal circuitry function was assessed using laminar, multichannel silicon probes specifically designed for recording from deep brain structures of large animals (pigs) (Ulyanova, Koch et al. 2018, Ulyanova, Cottone et al. 2019). Laminar oscillatory field potentials and single unit activity were examined and compared between injured and sham injured animals (under isoflurane anesthesia). Our data suggest that even a single concussion may alter both circuit-level and individual neuronal function in the hippocampus and may provide insight into aspects of cognitive dysfunction and hyperexcitability following concussion.

## Results

*Concussion Affects Electrophysiological Properties of Hippocampal CA1 Neurons.* To examine changes in hippocampal circuitry induced by concussion, *in vivo* electrophysiological recordings were obtained using 32-channel silicon probes that spanned the laminar structure of CA1 in the dorsal hippocampus (Figure 1A). These probes allowed recording of oscillatory activity in the local field potential across layers of CA1 and isolate single units using available spike sorting algorithms (see Methods) (Gold, Henze et al. 2006). Electrophysiological properties of CA1 neurons were compared in sham (n = 8, blue) and post-mTBI (n = 9, red) animals at 7 days post-concussion (Figure 1B). Total number of cells in sham ($n_{cells}$ = 125) and post-TBI ($n_{cells}$ = 93) groups were used for comparison between the groups. While the number of recorded cells per animal was not different between the groups (sham = 16 ± 3 cells vs. post-mTBI = 10 ± 3 cells, p = 0.24), the firing rate, spike width, and spike amplitude were all significantly reduced

in post-mTBI animals (Figure 1B). The firing rate of 4.43 ± 0.50 Hz in the sham animals was reduced to 2.09 ± 0.27 Hz in the post-mTBI animals ($p < 0.001$). The spike width of 0.358 ± 0.015 msec in the sham group was significantly reduced to 0.270 ± 0.008 msec in the post-mTBI group ($p < 0.0001$), and the spike amplitude was significantly reduced from 293 ± 27 μV in the sham group to 187 ± 27 μV in the post-mTBI group of animals ($p < 0.05$). In addition to firing single action potentials, neurons can also generate periods of rapid action potential spiking called burst firing, which are important for neural synchronization, neuronal coding, plasticity, and attention. Interestingly, the number of bursts per minute generated by hippocampal CA1 neurons was significantly reduced from 21 ± 3 bursts/min in the sham group to 8 ± 2 bursts/min in the post-mTBI group of animals ($p < 0.05$). These findings suggest that concussion may alter the intrinsic properties of CA1 neurons, which could affect their synchronization with hippocampal oscillations.

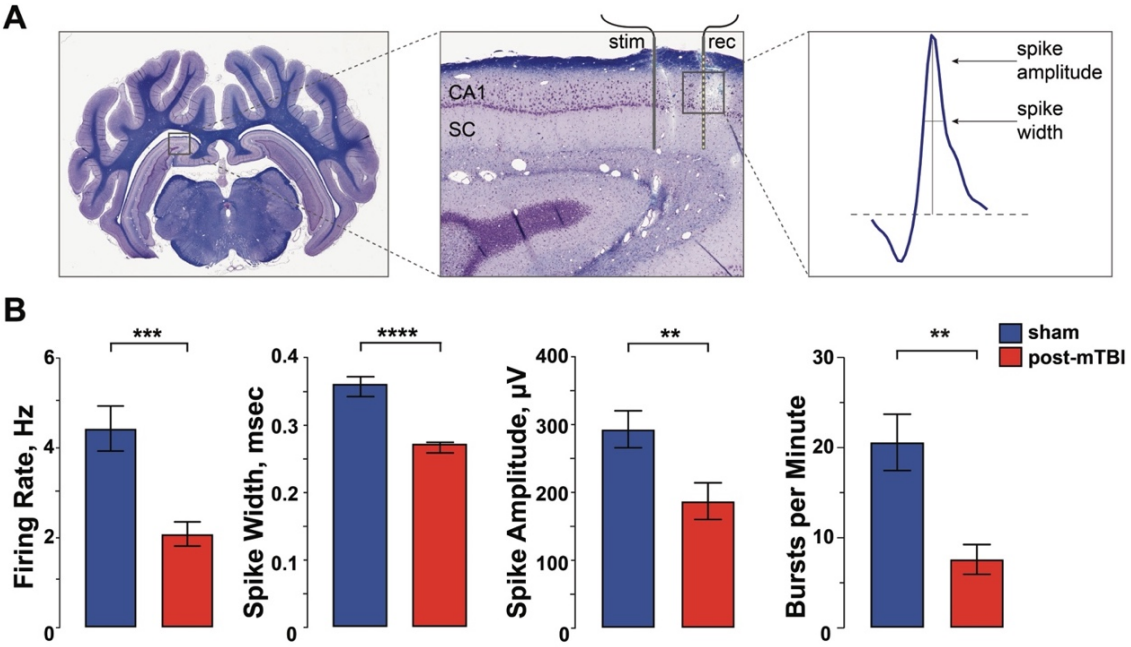


**Figure 1. Concussion Affects Electrophysiological Properties of Hippocampal CA1 Neurons.**
**A)** A representative coronal section through pig brain is shown on the left. Anatomical location of the stimulating (placed in the Schaffer collaterals, SC) and recording (placed in the hippocampal CA1 layer) electrodes are shown overlaid on the dorsal hippocampus (center panel). A representative example of action potential recorded with the silicone multichannel probe is shown on the right. **B)** At 7 days following mTBI, the firing rate of hippocampal CA1 neurons was significantly reduced in the sham (4.43 ± 0.50 Hz, blue) vs. post-mTBI (2.09 ± 0.27 Hz, red) groups of animals ($p < 0.001$). In addition, the spike width of 0.358 ± 0.015 msec recorded in the sham (blue) animals was significantly reduced to 0.270 ± 0.008 msec in the post-mTBI animals (red, $p < 0.0001$). The spike amplitude was also significantly reduced from 293 ± 27 μV in the sham (blue) animals to 187 ± 27 μV in the post-mTBI animals (red, $p < 0.05$). Moreover, the number of bursts per minute was significantly reduced from 21± 3 bursts/min in the sham (blue) animals to 8 ± 2 bursts/min in the post-mTBI animals (red, $p < 0.05$). Total number of cells recorded in the sham ($n_{cells} = 125$) and post-mTBI, groups of animals ($n_{cells} = 93$) were used for comparison between the groups. The number of the recorded cells per animal was not different between sham (16 ± 3 cells) vs. post-mTBI (10 ± 3 cells) groups ($p = 0.24$, not shown). Data presented as mean ± SEM.

*Pyramidal CA1 Neurons Preserve Their Firing Properties Following Concussion*. To further characterize the effects of mTBI on the hippocampal circuitry and to assess changes in specific subpopulations of cells in CA1, cells were separated (see Methods) into excitatory pyramidal cells (sham: $n_{pyr}$ = 49, post-mTBI: $n_{pyr}$ = 37; Figure 2A) and inhibitory interneurons (sham: $n_{int}$ = 52, post-mTBI: $n_{int}$ = 38; Figure 3A) (for review, see (Wheeler, White et al. 2015)). The firing probability and spike waveforms for putative CA1 pyramidal cells and CA1 interneurons were classified using previously published criteria for rodents (Csicsvari, Hirase et al. 1999, Broussard, Redell et al. 2020). Cells recorded at the bottom of the probe, which could be putative dentate granule cells, mossy cells, and interneurons in the dentate (sham: $n_{cells}$ = 14, post-mTBI: $n_{cells}$ = 5; not shown) as well as unclassifiable cells located throughout the length of the probe (sham: $n_{cells}$ = 10, post-mTBI: $n_{cells}$ = 16; not shown) were omitted from the analysis. The number of either pyramidal CA1 cells (sham = 7 ± 2 cells vs. post-mTBI = 4 ± 1 cells) or interneurons (sham = 6 ± 2 cells vs. post-mTBI = 4 ± 2 cells) per animal was not different between the sham and post-mTBI groups (pyramidal CA1 cells: p = 0.35; CA1 interneurons: p = 0.43).
While some observed changes in the electrophysiological properties of the putative pyramidal CA1 cells in the post-mTBI group trended towards significance (e.g., spike width), they were not significantly different from the sham group at 7 days following concussion (Figure 2B). Specifically, firing rate (sham = 2.27 ± 0.25 Hz vs. post-mTBI = 1.70 ± 0.27 Hz; p = 0.13), spike width (sham = 0.336 ± 0.022 msec vs. post-mTBI = 0.280 ± 0.014 msec; p = 0.05), spike amplitude (sham = 256 ± 36 μV vs. post-mTBI = 238 ± 50 μV; p = 0.76), and the number of bursts per minute (sham = 11 ± 2 bursts/min vs. post-mTBI = 9 ± 2 bursts/min; p = 0.44) were not significantly different between the sham (n = 8) and post-mTBI (n = 9) groups of animals (Figure 2B).

To examine whether pyramidal CA1 cells continue to interact with hippocampal oscillations properly following concussion, entrainment of pyramidal CA1 cells to local field potentials was investigated in the frequency range of 1 – 300 Hz, which includes theta, gamma, and ripple frequencies, all central to hippocampal function (Figure 2C). Notably, entrainment strength of pyramidal CA1 cells to the local gamma oscillation was significantly reduced in the 62 - 82 Hz frequency band (sham = 0.020 ± 0.005 vs. post-

mTBI = 0.012 ± 0.005, $p < 0.01$) and in the 103 - 117 Hz frequency band (sham = 0. 018 ± 0.006 vs. post-mTBI = 0.003 ± 0.001, $p < 0.05$). Additionally, we found a significant reduction in gamma power (35 – 75 Hz) detected locally to pyramidal CA1 cells (Figure 2D, $p < 0.01$). These results indicate that concussion disrupts the generation of gamma oscillations detected in the pyramidal cell layer, either due to the changes in the afferent inputs coming into CA1 or changes in local CA1 pyramidal cell-interneuron or interneuron-interneuron networks.

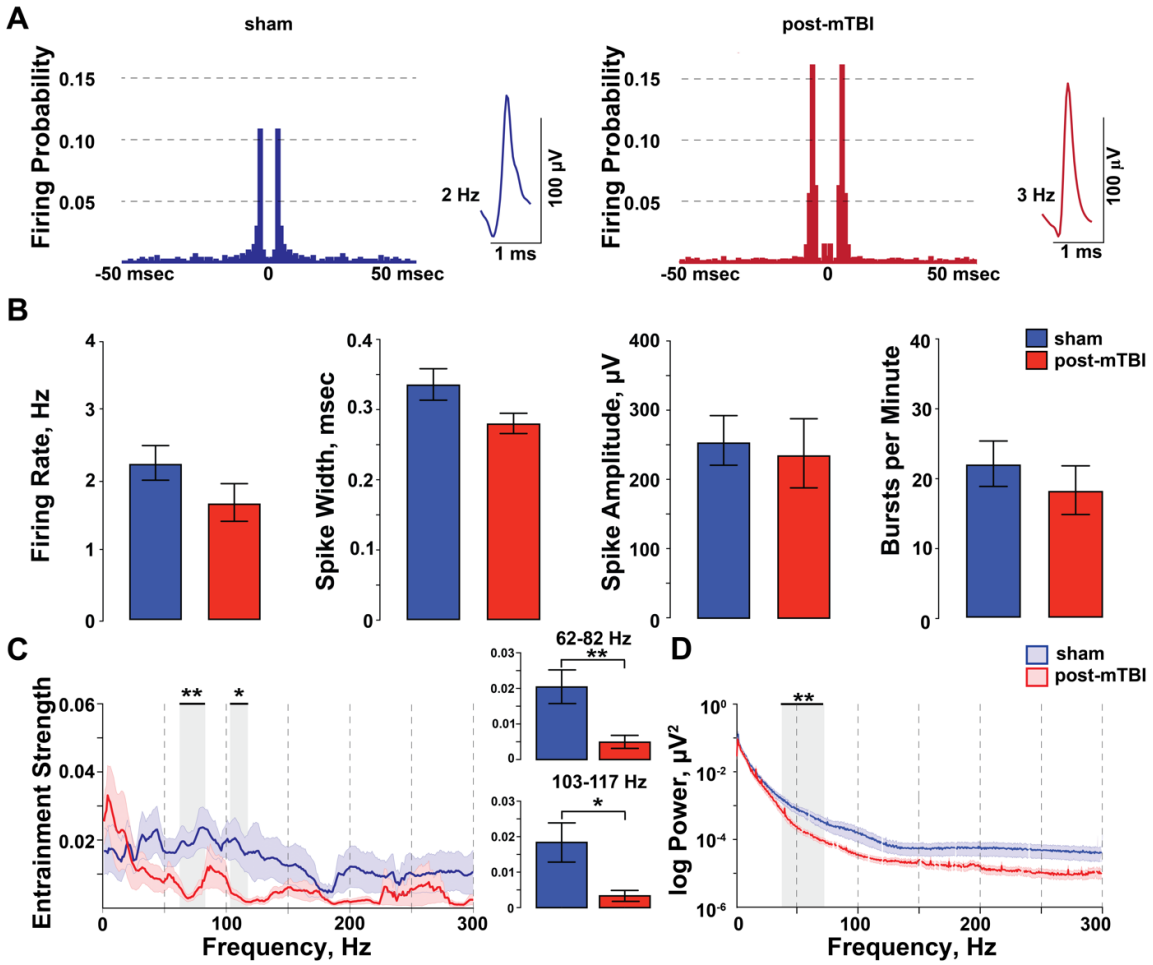


**Figure 2. Pyramidal CA1 Neurons Preserve Their Firing Properties Following Concussion.**
**A)** Representative examples of putative pyramidal CA1 cells from the sham (blue, left panel) and post-mTBI (red, right panel) animals are shown. Total number of putative pyramidal CA1 cells recorded in sham ($n_{pyr}$ = 49) and post-mTBI ($n_{pyr}$ = 37) animals was used for comparison between the groups. The number of pyramidal CA1 cells per animal (sham = 7 ± 2 cells vs. post-mTBI = 4 ± 1 cells) was not significantly different between the groups ($p = 0.35$, not shown). **B)** Electrophysiological properties of pyramidal cells were not changed 7 days following mTBI. The parameters analyzed include firing rate (sham = 2.27 ± 0.25 Hz, vs. post-mTBI = 1.70 ± 0.27 Hz; $p = 0.13$), spike width (sham = 0.336 ± 0.022 msec vs. post-mTBI = 0.280 ± 0.014 msec; $p = 0.05$), spike amplitude (sham = 256 ± 36 µV vs. post-mTBI = 238 ± 50 µV; $p = 0.76$), and number of bursts per minute (sham = 11 ± 2 bursts/min vs. post-mTBI = 9 ± 2 bursts/min; $p = 0.44$). **C)** Entrainment of pyramidal CA1 cells to local hippocampal oscillations was significantly decreased in the 62 - 82 Hz ($p < 0.01$) and the 103 - 117 Hz ($p < 0.1$) frequency ranges in the post-mTBI animals. **D)** Power spectral density analysis shows a significant decrease in the 35 – 75 Hz frequency range ($p < 0.01$) following mTBI. Noise associated with 60-Hz cycle was removed manually. Data presented as mean ± SEM.

*Inhibitory CA1 Interneurons Are Preferentially Affected Following Concussion.* Analysis of putative CA1 interneurons revealed that their electrophysiological properties were significantly altered at 7 days post-concussion (Figure 3B). In contrast to pyramidal CA1 cells, CA1 interneurons had a significantly reduced firing rate (sham = 7.46 ± 1.0 Hz vs. post-mTBI = 3.01 ± 0.55 Hz, $p < 0.001$), spike width (sham = 0.373 ± 0.022 msec vs. post-mTBI = 0.263 ± 0.009 msec, $p < 0.001$), and spike amplitude (sham = 367 ± 50 μV vs. post-mTBI = 170 ± 43 μV, $p < 0.01$). Notably, the firing rate of CA1 interneurons decreased as a rotational velocity increased, changing significantly from 7.46 ± 1.0 Hz in sham animals (n = 8) to 3.78 ± 0.93 Hz in animals injured at ~190 rad/sec (188 ± 11 rad/sec, n = 4), and further to 2.33 ± 0.0.51 Hz in animals injured at ~260 rad/sec (256 ± 7 rad/sec, n = 5) ($p < 0.05$, not shown). In addition, the number of bursts per minute was significantly reduced in post-mTBI animals (sham = 33 ± 7 bursts/min vs. injury = 9 ± 4 bursts/min, $p < 0.01$). Since electrophysiological properties of pyramidal CA1 cells were not substantially altered (Figure 2B), these results indicate that CA1 interneurons are preferentially affected at 7 days following a single inertial injury. Notably, entrainment of CA1 interneurons to the hippocampal theta oscillation (4 - 6 Hz) was significantly increased 7 days post-concussion (sham = 0.013 ± 0.005 vs. post-mTBI = 0.041 ± 0.014, $p < 0.05$). Additionally, there was a significant reduction in the power of high frequency oscillations (frequency range = 80 – 300 Hz) detected locally to interneurons (but not pyramidal) CA1 cells, potentially due to the observed reduction in the firing rate of CA1 interneurons or desynchronization of the CA1 network (Figure 3C, $p < 0.1$). These results indicate that concussion alters intrinsic and/or synaptic properties of CA1 interneurons, which affects local gamma and high-frequency oscillations presumably generated by local CA1 interneurons. These changes likely alter the way pyramidal CA1 cells interact with local hippocampal oscillations.

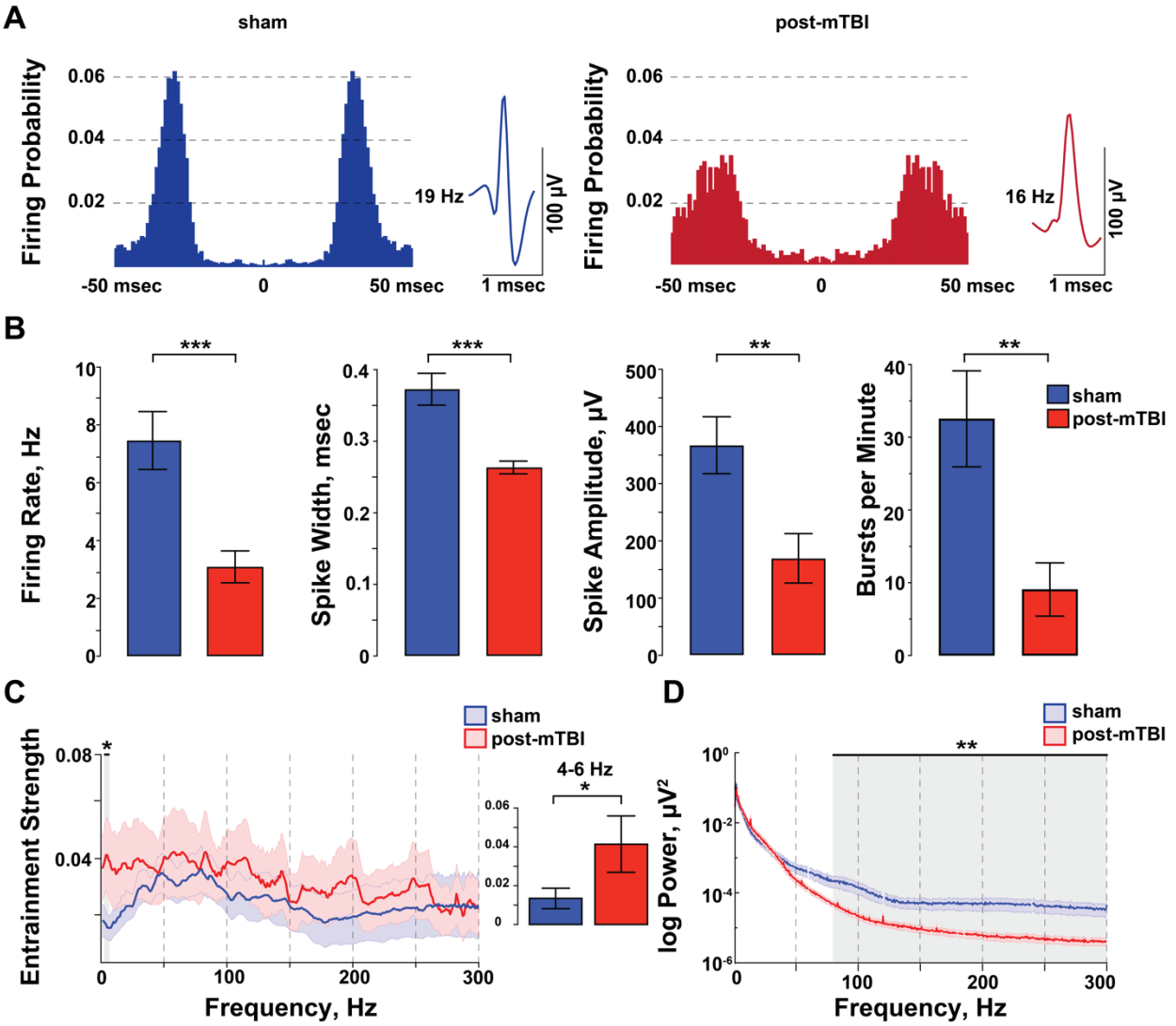


**Figure 3. Inhibitory CA1 Interneurons Are Preferentially Affected at 7 Days Following Concussion.** **A)** Representative examples of CA1 interneurons from sham (blue, left panel) and post-mTBI (red, right panel) animals. Total number of CA1 interneurons recorded in sham ($n_{int}$ = 52) and post-mTBI ($n_{int}$ = 38) animals were used for comparison between the groups. The number of CA1 interneurons per animal (sham = 6 ± 2 cells vs. post-mTBI = 4 ± 2 cells) were not significantly different between the groups ($p = 0.43$, not shown). **B)** Electrophysiological properties of CA1 interneurons were significantly altered 7 days post inertial injury. Firing rate of CA1 interneurons was significantly reduced from 7.46 ± 1.0 Hz in sham animals (blue) to 3.01 ± 0.55 Hz (red) in post-mTBI animals ($p < 0.001$). The spike width was significantly reduced from 0.373 ± 0.022 msec in sham animals (blue) to 0.263 ± 0.009 msec in post-mTBI animals (red) ($p < 0.001$). Spike amplitude was also significantly reduced from 367 ± 50 µV in sham animals (blue) to 170 ± 43 µV in post-mTBI animals ($p < 0.01$). In addition, number of bursts per minute was significantly reduced following concussion (sham = 33 ± 7 bursts/min vs. injury = 9 ± 4 bursts/min, $p < 0.01$). **C)** Entrainment of CA1 interneurons to local hippocampal oscillations was significantly increased in the 4 - 6 Hz frequency range ($p < 0.1$). **D)** Power of the high frequency oscillations was significantly decreased in the 80 - 300 Hz frequency range ($p < 0.01$). Noise associated with 60-Hz cycle was removed manually. Data presented as mean ± SEM.

*Hippocampal Hyperexcitability Post-Concussion.* Reduced excitability of GABAergic inhibitory interneurons without a corresponding change in the activity of excitatory neurons in the hippocampus has been previously linked to hippocampal hyperexcitability

(Toth, Hollrigel et al. 1997, Witgen, Lifshitz et al. 2005, Hunt, Scheff et al. 2011, Pavlov, Scimemi et al. 2011). Moreover, the differential response to varying stimulation intensities in slices previously reported between sham and post-mTBI animals using this model (Wolf, Johnson et al. 2017), further suggests hyperexcitability in hippocampus post-concussion. Therefore, we used electrical stimulation of the Schaffer collateral inputs coming into the CA1 layer from the CA3 (sham = 3, post-mTBI = 8) as described previously to assess changes in the excitability levels of the intact brain (Ulyanova, Koch et al. 2018). Representative examples of the evoked laminar field potentials in dorsal CA1 with Schaffer collateral stimulation are shown for a sham (blue, left panel) and a post-mTBI (red, right panel) animals (Figure 4A). During a series of the paired-pulse (PP) stimulations in the Shaffer collaterals (inter-pulse interval of 30 msec, 20 repeats, 5 sec apart), a sustained depolarization over 1 sec long was observed in a subset (n=2 out of 5) of animals injured at ~260 rad/sec (Figure 4B). Notably, this depolarizing shift was detected across all hippocampal layers and has features similar to the paroxysmal depolarizing shift previously observed in epileptic brain (for review, see (Hotka and Kubista 2019)). In the example shown in Figure 4B, the depolarizing shift happened approximately 4 sec post the third PP stimulation and continued for over 1 sec, overlapping with the fourth PP stimulation. During prolonged depolarization, an increase in the multi-unit activity was also observed in some hippocampal layers (Figure 4C). In addition, depolarization was followed by a loss of synaptic responses to PP stimulation (Figure 4D). Other forms of hippocampal hyperexcitability such as paroxysmal rhythmic spikes were observed in the form of synchronized activity in the 6 - 8 Hz frequency range across all laminar layers in injured but not sham animals (Figure 4D). Interestingly, paroxysmal rhythmic spikes were also present during baseline recordings in all post-mTBI (n = 9) but not sham (n = 8) animals (not shown), potentially suggesting increased hyperexcitability and synchronization of hippocampal circuitry prior to the introduction of a stimulus.

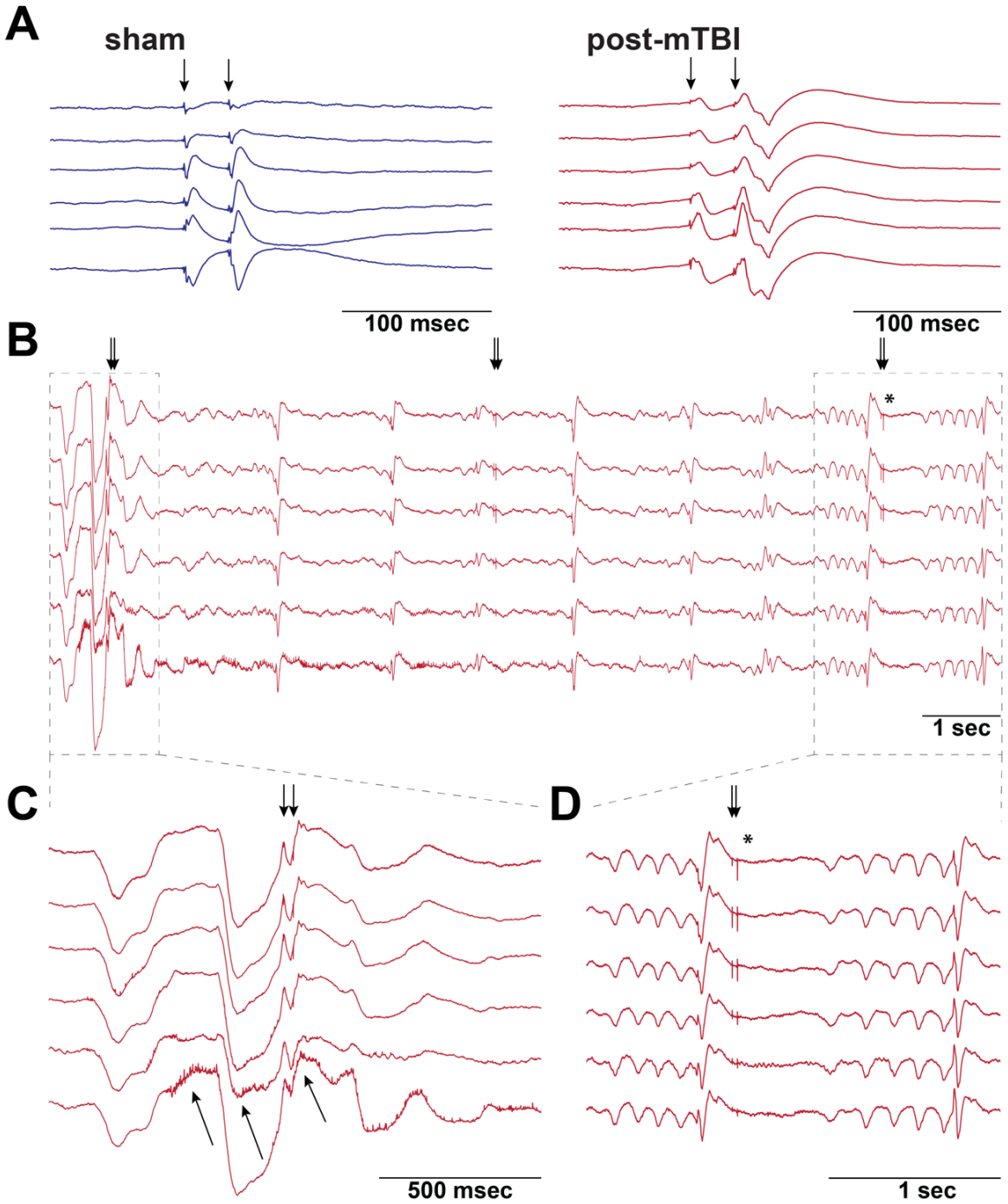


**Figure 4. Hippocampal Hyperexcitability Post-Concussion.**

**A)** Representative oscillatory laminar field responses to a stimulation in Schaffer Collaterals (arrows) are shown in the CA1 pyramidal cell layer for a sham (blue, left panel) and post-mTBI (red, right panel) animals. **B)** A depolarizing shift was observed in a subset (n = 2) of post-mTBI (but not sham) animals during paired pulse (PP) stimulation. In this example, the depolarizing shift happened approximately 4 sec post the third PP stimulation and continued for over 1 sec, overlapping with the fourth PP stimulation (top arrows). PP stimulation is shown with arrows (inter-pulse interval, IPI = 30 msec, 20 repeats, with 5 sec in between consecutive stimulations). **C)** During prolonged depolarization, an increase in the multi-unit activity was also observed in some hippocampal layers (bottom arrows). **D)** A prolonged depolarization followed by a loss of synaptic responses to PP stimulation (arrows) was also observed in all layers of hippocampus (asterisk). In addition, other forms of hippocampal hyperexcitability such as paroxysmal rhythmic spikes in the form of synchronized activity in the 6 - 8 Hz frequency range across all laminar layers were observed in all post-mTBI (n=9) but not sham (n=8) animals.

*Model of Parvalbumin-Positive ($PV^+$) CA1 Interneurons Reveals Potential Dysfunction of Sodium Channels.* Interneurons in the hippocampus are involved in the generation of gamma oscillations and provide input-specific inhibition to pyramidal cells via feedforward and feedback inhibition (Soltesz and Deschenes 1993, Mann, Suckling et al. 2005, Buzsáki and Wang 2012). Specifically, it has been previously shown that parvalbumin-positive ($PV^+$) basket cells provide peri-somatic, feedforward inhibition in the hippocampal CA1 region (for review, see (Klausberger and Somogyi 2008, Pelkey, Chittajallu et al. 2017)). These cells stabilize hippocampal circuitry during changes in input and control the selection of cell ensembles by allowing only certain number of pyramidal cells to fire in response to the stimulus (for review, see (de Almeida Licurgo 2009, Buzsáki and Wang 2012, Rennó-Costa, Teixeira et al. 2019)). Interestingly, pathological changes in $PV^+$ interneurons in CA1 have been also shown to play a crucial role in the development of epilepsy (Yu, Mantegazza et al. 2006, Ogiwara, Miyamoto et al. 2007). To elucidate potential mechanisms underlying the electrophysiological changes observed in CA1 interneurons in our animal model of concussion, we used the NEURON simulation environment (Hines and Carnevale 1997, Hines and Carnevale 2001), specifically a model of hippocampal $PV^+$ basket cells described previously (Bezaire, Raikov et al. 2016), and adjusted parameters to fit the observed decrease in spike size and firing rate observed in interneurons of mTBI animals. The full individual parameter spaces of the CA1 interneuronal model were altered by hand without an *a priori* hypothesis in both the soma and dendrites to examine whether changing multiple parameters might fit the reduced firing rate, spike width and spike amplitude observed in CA1 interneurons post-mTBI (Figure 5). The best fit between model-generated values (Figure 5A, green) and experimental data of injured CA1 interneurons (Figure 5A, red) was achieved by changing the inactivation of voltage-gated sodium channels ($h_{inf}$) in the model (Summary Table 1). The model suggests that the experimental data is best described by a negative shift of $h_{inf}$ towards more hyperpolarized voltages, with the midpoint of the steady state inactivation curve changing from –35 mV to –44.5 mV (Figure 5B, arrow). Under these modeling conditions, the window current of voltage-gated sodium channels, defined as an overlap between the activation ($m_{inf}$) and inactivation ($h_{inf}$) curves, is decreased by ~30% following inertial injury. The best fit for the $PV^+$ interneuron model corresponds to

a similar decrease in firing rate (model = 60% vs. experimental data = 59%), spike width (model = 28% vs. experimental data = 29%), and spike amplitude (model = 27% vs. experimental data = 54%). The model output using the best fit parameters is shown in Figure 5C. These results suggest that pathological changes in the inactivation of voltage-gated sodium channels may be a potential mechanism for $PV^+$ interneuron dysfunction post-mTBI.

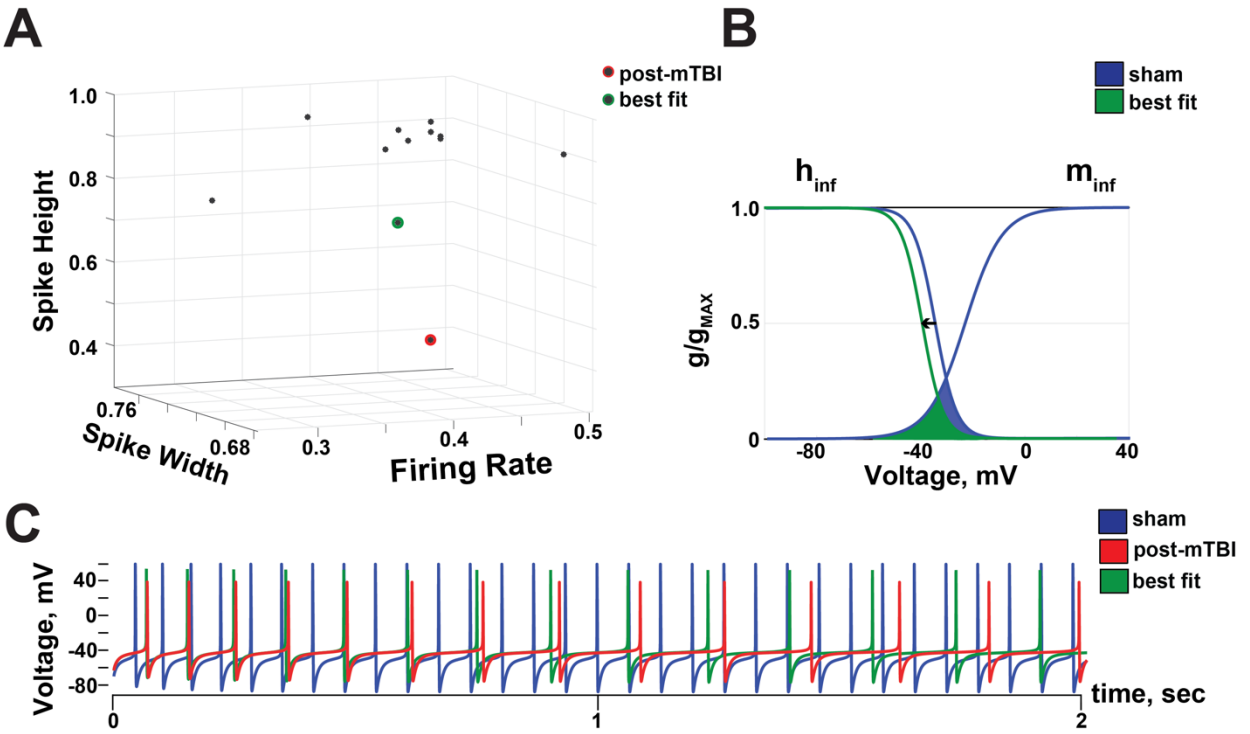


**Figure 5. Model of Basket Cells Reveals Potential Dysfunction in Sodium Channels.**
**A)** NEURON environment was used to model parvalbumin-positive ($PV^+$) CA1 interneurons. The original parameters were altered in both the soma and dendrites to match experimental data from post-mTBI animals (red dot). The best fit (green dot) corresponds to a 60% reduction in the interneuronal firing rate (vs. 59% in the experimental data), a 28% in the spike width (vs. 29% in the experimental data), and a 27% reduction in the spike amplitude (vs. 54% in the experimental data). **B)** Voltage dependence of activation ($m_{inf}$, right curve) and steady-state inactivation ($h_{inf}$, left curve) of sodium currents generated in the model $PV^+$ CA1 interneuron. A best fit to the experimental data is produced by a negative shift of the inactivation ($h_{inf}$) from –35 mV (blue) to –44.5 mV (green) and is shown with an arrow. Activation ($m_{inf}$) was not altered when using the best fit parameters. At these bets fit parameters, the window current of voltage-gated sodium channels (area under the curves) is decreased by ~ 33% (green). **C)** Changes in firing rate and spike amplitude are shown for sham (blue), post-mTBI (red), and best fit parameters (green).

| Diffuse Axonal Injury, Experimental Data | Firing Rate Factor | Spike Width Factor | Spike Amplitude Factor |
|---|---|---|---|
| | 0.41 | 0.71 | 0.46 |
| **Condition (NEURON PV+ Interneuron Model)** | **Firing Rate Factor** | **Spike Width Factor** | **Spike Amplitude Factor** |
| **thinf = -59** | **0.40** | **0.72** | **0.73** |
| thinf = -60 | 0.26 | 0.71 | 0.82 |
| thinf = -59.5; ena = 80 | 0.39 | 0.70 | 0.97 |
| thinf = -57, sh = 15.5, ena = 80, gmaxKdrfast = 0.026 | 0.42 | 0.73 | 1.08 |
| thinf = -57, sh = 15.5, gmaxKdrfast = 0.026 | 0.39 | 0.77 | 0.93 |
| thinf = -58, ena = 70, gmaxKdrfast = 0.026 | 0.48 | 0.68 | 0.92 |
| thinf = -59.3, ena = 80 | 0.42 | 0.71 | 0.98 |
| dendrites 1, 2 = 70, thinf = -59.3 | 0.42 | 0.74 | 0.88 |
| dendrites 0, 1, 2, 3: ena = 65; thinf = -59.3 | 0.45 | 0.74 | 0.90 |
| dendrites 0,1 = ena 65; 2,3 = ena 70; thinf to -59.3 | 0.45 | 0.74 | 0.91 |
| dendrites 0,5,10,13: ena = 60; thinf = -59.3 | 0.42 | 0.73 | 0.91 |
| dendrites 0,5,10,13: ena = 65; thinf = -59.5 | 0.42 | 0.71 | 0.95 |

**Summary Table 1. NEURON-simulation environment model of parvalbumin-positive ($PV^+$) CA1 interneurons.** Model parameters used to simulate experimental conditions (red) observed in CA1 interneurons at 7 days following mTBI. The model suggests that the experimental data is best described by a negative shift of $h_{inf}$ (the slope of the inactivation gate of voltage-gated sodium channels) towards more hyperpolarized voltages. At this condition, the midpoint of the steady state inactivation curve changes from –35 mV to –44.5 mV.

## Discussion

Concussion (or mild TBI) is a prevalent type of brain injury, with the potential for long-term consequences. The lifetime prevalence for teenagers in the US was recently reported to be almost 25%, and annual incidence for all ages was reported at 1.2% of the population (Langer, Levy et al. 2020, Veliz, McCabe et al. 2021). Rates of concussion among the military population are even higher, with over 240,000 diagnosed concussions in the active military between years of 2000-2015 (Helmick, Spells et al. 2015). Concussion can produce long-lasting cognitive deficits, which manifest as poor performance in tests of memory, learning, and delayed recall up to several weeks post injury (Anita, Lori et al. 2008, Giza, Greco et al. 2018, de Freitas Cardoso, Faleiro et al. 2019). The hippocampus is involved in learning and memory (Carr, Jadhav et al. 2011), and its role in integrating information may be particularly sensitive to timing disruptions associated with axonal injury or disruptions in oscillatory activity (for review, see (Wolf and Koch 2016)). The hippocampal CA1 region plays an essential role in the acquisition and consolidation of spatial and episodic memories by integrating oscillatory information coming in via entorhinal and CA3 axonal inputs and by supporting the encoding and

retrieval of hippocampus-dependent memories (Hazan, Zugaro et al. 2006, Singh, Meier et al. 2014, Koch, Cottone et al. 2020, Levin, Temkin et al. 2021).

Studies on electrophysiological changes following clinical concussion are sparse due to the lack of data sets collected on human patients acutely or over time post-concussion (for review, see (Schmitt and Dichter 2015)). Changes in neuronal firing and local hippocampal oscillations have been reported in rodent models of mTBI, potentially suggesting abnormalities in temporal coding, a crucial element of episodic memory formation and encoding (Paterno, Metheny et al. 2015, Broussard, Redell et al. 2020, Ondek, Pevzner et al. 2020). However, large animal gyrencephalic models offer several advantages in modelling the complex biomechanics and resultant pathophysiology of inertial injury, and may be the most relevant for understanding the effects of concussion on regions underlying cognitive processing and memory. We have previously reported changes in hippocampal circuitry following mTBI using an *ex vivo* slice paradigm (Wolf, Johnson et al. 2017). In the current study, we advanced our investigation of electrophysiological changes in the hippocampal CA1 circuitry following rotational acceleration injury in the intact anesthetized swine at 7 days post-mTBI using high-density laminar electrophysiology. We found that action potential recordings from the CA1 interneurons had a significantly decreased firing rate, amplitude, width, and burst occurrence in the injured compared to the control animals, while action potential recorded from the CA1 pyramidal cells were unchanged. Moreover, we found that concussion caused hippocampal hyperexcitability *in vivo*, potentially due to synaptic dysfunction and disrupted neuronal communication between the CA1 pyramidal cells and interneurons, which confirms findings from prior work utilizing this model (Wolf, Johnson et al. 2017). These identified changes may underlie aspects of cognitive disruption following mTBI.

*CA1 Interneurons are Preferentially Affected by Concussion.* We found that concussion-induced neuronal changes in the hippocampus were cell-type specific and only affected CA1 interneurons. We showed that concussion induced by inertial rotation led to changes in firing rate and pattern as well as spike shape exclusively in CA1 interneurons and not pyramidal cells. Specifically, CA1 interneurons had decreased firing rate and bursting at

7 days following concussion, indicating a significant decrease in the inhibition. This may potentially lead to an increase in the excitation and, hence, hyperexcitability in the CA1 hippocampal layer. Our NEURON modeling results indicated that the decreased firing rate and a reduction in spike amplitude and width observed in CA1 interneurons of mTBI animals may be due to a negative shift in the inactivation of voltage-gated $Na^+$ channels. While other groups have proposed a coupled left-shift of activation/availability of sodium channels using the *in vitro* model of stretch injury (Boucher, Joós et al. 2012), our model did not predict this negative shift in sodium channel activation but instead predicted a negative shift in sodium channel inactivation. Notably, pathological changes affecting the inactivation of voltage-gated $Na^+$ channels have been previously reported following injury (Wolf, Stys et al. 2001, Iwata, Stys et al. 2004). Using an *in vitro* model of axonal stretch injury, we previously demonstrated that traumatic deformation of axons induced abnormal sodium influx through TTX-sensitive $Na^+$ channels, leading to an increase in the intracellular $Ca^{2+}$ concentration in axons (Wolf, Stys et al. 2001). Furthermore, axonal stretch injury induced structural changes in the alpha-subunit of voltage-gated sodium channels and led to changes in sodium channel inactivation, followed by a long-term increase in the intracellular $Ca^{2+}$ and subsequent proteolysis of the sodium channel alpha subunit (Iwata, Stys et al. 2004).

Stronger entrainment of CA1 interneurons to local theta oscillation observed at 7 days following concussion may also suggest a potential shift in the recruitment/activation of CA1 interneuron subpopulations (Pike, Goddard et al. 2000, Gloveli, Dugladze et al. 2005). $PV^+$ CA1 interneurons (specifically basket cells) are directly involved in feedforward inhibition and have been proposed to stabilize the frequency of local gamma oscillations and maintain a sparsity of neuronal ensembles in the presence of changes in the excitatory drive (de Almeida Licurgo 2009, Buzsáki and Wang 2012, Rennó-Costa, Teixeira et al. 2019). This observation may further support TBI associated disruptions in feedforward inhibition provided by $PV^+$ interneurons in CA1. This disruption may also impair behavioral tasks requiring network sparsity, such as pattern separation, that have been previously reported to be disrupted in a rodent model of mTBI (Munyon, Eakin et al. 2014). Concussion leading to interneuronal changes may underscore the importance of

cognitive tasks that rely on spatiotemporal precision for clinical diagnosis. However, testing this hypothesis may require awake behaving electrophysiology and developing behavioral tasks sensitive to this injury (Ulyanova, Cottone et al. 2019).

It is worth highlighting that the methods used to distinguish putative CA1 interneurons from putative CA1 pyramidal cells were developed in the rat hippocampus and are here adapted to the porcine hippocampus for the first time. We localized the pyramidal cell layer based on a mapping technique we developed in the pig to place multi-channel silicon probes in CA1 (for details, see (Ulyanova, Koch et al. 2018)). Only single units located within the pyramidal cell layer (the top portion of silicon probe) were selected for analysis. To identify hippocampal CA1 cells as either putative pyramidal cells or interneurons within this layer, we utilized protocols previously described in the rat (Csicsvari, Hirase et al. 1999, Broussard, Redell et al. 2020). Electrophysiological characteristics that define spike shape and firing/bursting properties of pig hippocampal neurons may vary from those defining rodent CA1 neurons due to the differences in the size of neurons as well as variability in the expression of synaptic proteins and voltage-gated channels responsible for the generation of action potentials (Sengupta, Faisal et al. 2013). In addition, we have previously characterized the CA1 stratum pyramidale and stratum radiatum layers demonstrating that they are significantly larger in pigs than in rodents, and have described a progressive dispersion of pyramidal cells leading to a less densely packed pyramidal layer (Ulyanova, Koch et al. 2018). This dispersion has the effect of partially blurring the distinction between stratum pyramidale and the most dorsal aspects of stratum radiatum, as synaptic inputs into the dendritic tree of the more dorsally located cells will colocalize with the more ventrally located cell bodies. Also, anesthesia has been known to affect neuronal firing rate as well as the pattern and strength of inputs arriving into the dendritic arbor of the CA1 pyramidal cells (Lustig, Wang et al. 2015). These caveats notwithstanding, given other similarities between porcine and rodent hippocampal electrophysiology such as comparable laminar power profiles of classic hippocampal oscillations (theta, gamma and ripple band frequencies), as well as comparable CA1 neuron autocorrelograms (Ulyanova, Koch et al. 2018), we believe these established CA1

sorting techniques are reasonably applied in our study despite the novelty of their use in the porcine hippocampus.

*Pyramidal CA1 Cells Are Desynchronized with Respect to Important Organizing Oscillations.* Although we found no alterations in intrinsic properties, we demonstrated that CA1 pyramidal cells lose their synchronization with local gamma oscillations at 7 days following concussion. Previously, we identified a laminar profile of overall oscillations detected in the pig hippocampus (Ulyanova, Koch et al. 2018). Here, we observed a significant reduction in gamma oscillation (35 – 75 Hz) power detected locally to the pyramidal CA1 cells post-concussion. The reduction in low gamma oscillations (35 – 55 Hz) could be due to a decrease in the fiber volleys of Schaffer collaterals (inputs from the CA3 layer) previously reported in this model (Wolf, Johnson et al. 2017). Taking into account the fact that networks of interneurons in CA1 support the generation of local high gamma oscillations (55 - 75 Hz) and entrain CA1 pyramidal cells to these oscillations (for review, see (Colgin and Moser 2010, Buzsáki and Wang 2012)), these results could also indicate that either CA1 interneurons are preferentially affected by inertial injury or that they have not fully recovered by 7 days following concussion. Loss of entrainment of CA1 pyramidal cells to gamma oscillations may underlie aspects of post-concussive syndrome (for review, see (Wolf and Koch 2016)), but oscillatory activity is influenced by anesthesia, so these results need to be confirmed in the awake behaving animal.

*Hippocampal CA1 Layer Is Hyperexcitable.* In this study, we were able to implement *in vivo* electrophysiology in the post-concussion pig using multichannel laminar probes spanning the layers of the porcine hippocampus (Ulyanova, Koch et al. 2018, Ulyanova, Cottone et al. 2019). We observed spontaneous depolarizing shifts in a subset of injured animals (2 out of 9), which have been detected on the multichannel laminar probe across all layers of hippocampus and were followed by a loss of synaptic responses to stimulation. In the literature, the paroxysmal depolarizing shift (PDS) is described as a prolonged, large-amplitude positive shift of membrane voltage, during which a spike generation would progressively decrease in amplitude until only small oscillations remained riding on top of the PDS. In epilepsy, paroxysmal depolarizing shift and

spreading depolarization have been observed in hippocampus and cortex using animal models as well as in human patients (for review, see (Hotka and Kubista 2019)). In TBI research, spontaneously generated paroxysmal depolarizations have been only detected in organotypic hippocampal cultures following long-term activity deprivation, potentially due to a homeostatic plasticity mechanism (Koch, Huh et al. 2010). Therefore, the prolonged depolarizing shift observed using our model of concussion is the first such epileptogenic event described in the *in vivo* preparation. A long-lasting depolarization shift accompanying the repetitive action potentials upon paired-pulse stimulation of Schaffer collaterals could be due to changes in fiber volleys, given the differential response to varying stimulation intensities in slice previously reported between sham and injured animals using this model (Wolf, Johnson et al. 2017). In the current study, all layers of the dorsal hippocampus were undergoing the prolonged depolarizations synchronously. Additionally, we also observed recurring paroxysmal oscillatory events in the form of arcuate spikes occurring in a synchronized manner across all hippocampal layers in all post-mTBI but not sham animals. Similar epileptogenic spikes have been previously reported after experimental TBI in rodent models and are thought to reflect repeated population spikes associated with hypersynchronous multi-unit discharges (Bragin, Li et al. 2016). Therefore, there are potentially multiple pathological mechanisms involved in the generation of the prolonged depolarizations since we are looking at different inputs to the CA1 dendritic arbor simultaneously with these laminar probes.

*Concussion as a Risk for Development of Post-Traumatic Epileptogenesis.* Concussion has been previously identified as a risk factor for the development of epilepsy (for review, see (Agrawal, Timothy et al. 2006)). However, mechanisms underlying the development of post-traumatic epileptogenesis (PTE) post-concussion have not yet been identified. Here, we reported a significant reduction in the power of high frequency oscillations (80 – 300 Hz) detected locally to interneurons (but not pyramidal) CA1 cells, which may be due to the observed reduction in the firing rate of CA1 interneurons or desynchronization of the CA1 network. A reduction in the number of hippocampal interneurons is a major pathology associated with the development of unprovoked seizures both in experimental models and in human temporal lobe epilepsy (Huusko, Römer et al. 2015). While

interneuronal cell loss in our porcine inertial injury model has not been histologically assessed, the number of electrophysiologically active cells recorded in our model was not significantly different between the sham and injured animals. Nevertheless, changes in the electrophysiological properties of interneurons may affect circuit level hippocampal interactions and increase the risk for hyperexcitability and epileptogenesis.

Hippocampal CA1 hyperexcitability and epileptogenesis caused by changes in the sodium channel expressed in inhibitory $PV^+$ interneurons have been previously reported (Liautard, Scalmani et al. 2013). While histological and electrophysiological studies have previously identified $PV^+$ interneurons to be selectively altered in experimental models of rodent TBI (Nichols, Bjorklund et al. 2018, Carron, Sun et al. 2020, Figueiredo, Harbert et al. 2020, MacMullin, Hodgson et al. 2020), we could not identify a specific sodium channel responsible for the observed changes in CA1 interneurons following concussion. Using NEURON model of a CA1 $PV^+$ interneuron (specifically basket cell), we observed a reduction in the sodium channel window current which in turn may also affect resurgent and/or persistent currents generated by voltage-gated sodium channels (for review, see (Eijkelkamp, Linley et al. 2012)). Interestingly, changes in the window current of voltage-gated sodium channels have been previously reported in epilepsy (for review, see (Mantegazza, Curia et al. 2010, Catterall 2018)). Potential mechanisms for the negative shift of sodium channel inactivation include altered properties of sodium channel auxiliary subunits (beta (Spampanato, Kearney et al. 2004) and gamma subunits) as well as the involvement of slow inactivation caused by prolonged depolarization (Vilin and Ruben 2001), both of which were proposed to play a crucial role in sodium channel associated epilepsies (Catterall 2018).

In summary, using a translational, large animal model of concussion we have demonstrated that a single inertial injury alters hippocampal circuitry at 7 days post-injury by affecting the electrophysiological properties of CA1 neurons. In particular, the physiological properties of interneurons in CA1 are substantially altered following concussion. These interneuronal alterations may be due to a change in the inactivation of voltage-gated sodium channels expressed in somata of $PV^+$ basket cells, as suggested

by the exhibited decrease in local gamma power and the loss of entrainment of pyramidal cells to local gamma oscillations. We also observed hippocampal hyperexcitability in the local field potentials predominantly following stimulation. These changes may underlie aspects of cognitive dysfunction following concussion, as well as increase the risk for PTE (Lolk, Dreier et al. 2021). Future studies are needed to investigate if the changes in sodium channel function predicted by our model are observed experimentally. Further assessing these changes over time and determining the differential involvement of specific interneuron populations may reveal therapeutic targets for improving concussion induced memory dysfunction and/or epileptogenesis. Restoring GABAergic interneuronal function before hyperexcitability proceeds to epileptogenesis may improve cognitive outcomes and decrease seizure frequency, as has been previously demonstrated in a mouse model of PTE (Hunt, 2019). While it is unknown whether the observed changes in interneuronal function persist at time points greater than one week post-injury, pharmacological interventions centered on restoring sodium channel inactivation may be a new target for improving cognitive function following concussion.

## Materials and Methods

*Animal Care*: Yucatan miniature pigs (n = 17) were purchased from Sinclair and underwent the current studies at the age of 6 months and a mean weight of 27.7 ± 4.5 kg (mean ± stdev). The animals were fed standard pig chow and water ad libitum. All animals were pair housed when possible and were always in a shared room with other pigs in a research facility certified by the Association for Assessment and Accreditation of Laboratory Animal Care International (AAALAC facility). All experiments were conducted according to the ethical guidelines set by the Institutional Animal Care and Use Committee of the University of Pennsylvania and adhered to the guidelines set forth in the NIH Public Health Service Policy on Humane Care and Use of Laboratory Animals (2015).

*Surgical Procedures*: Prior to the procedures, animals were fasted for 16 hours with water remaining ad libitum. After induction with 20 mg/kg of ketamine (Hospira, 0409-2051-05) and 0.5 mg/kg of midazolam (Hospira, 0409–2596-05), anesthesia was provided with using 2-2.5% isoflurane (Piramal, 66794-013-25) via a snout mask and glycopyrrolate was given subcutaneously to curb secretions (0.01 mg/kg; West-Ward Pharmaceutical Corp., 0143-9682-25). The animals were intubated with a size 6.0 mm endotracheal tube and anesthesia was maintained with 2-2.5% isoflurane per 2 liters $O_2$. Heart rate, respiratory rate, arterial oxygen saturation, end tidal $CO_2$, blood pressure and rectal temperature were continuously monitored, while pain response to pinch was periodically assessed. All these measures were used to maintain an adequate level of anesthesia. A forced air warming system was used to maintain normothermia.

*Closed-Head Rotational Injury using the HYGE Pneumatic Actuator*: A mild form of TBI or concussion was produced as previously described (Johnson, Stewart et al. 2016, Johnson, Weber et al. 2018, Grovola, Paleologos et al. 2021). Briefly, the injury was performed under isoflurane anesthesia, while physiological parameters of the animals were being closely monitored. Closed-head rotational acceleration was performed using the HYGE pneumatic actuator, a device capable of producing non-impact head rotation (up to 110 degrees in less than 20 msec) with a controlled relationship between maximum rotational acceleration and injury severity (see (Cullen, Harris et al. 2016) for more details). Angular velocity was recorded using a magneto-hydrodynamic sensor (Applied Technology Associates, Albuquerque, NM) connected to a National Instruments DAQ, controlled by LabVIEW. The animal's head was secured to a padded bite plate under anesthesia and attached to the HYGE device. We utilized a coronal plane of rotation that induces a modest delay in return-of-consciousness post-injury (compared to anesthetized sham animals) and minimal subdural bleeding, but produces patterns of diffuse axonal injury, such as swellings in the form of discrete axonal bulbs and axonal varicosities observed at the roots of the cortical gyri, at the interface of the grey and white matter, and within the deep white matter (Johnson, Stewart et al. 2016, Johnson, Weber et al. 2018, Grovola, Paleologos et al. 2021, Wofford, Grovola et al. 2021). To induce a mild injury phenotype (concussion), a single rapid head rotation was performed within a range of

rotational velocities (168 – 269 rad/sec, n = 9), with the mean angular peak velocity being 226 ± 13 rad/sec. For a subset of analyses, the injured animals were divided into two subgroups, the animals injured at ~190 rad/sec (188 ± 11 rad/sec, n = 4) and the animals injured at ~260 rad/sec (256 ± 7 rad/sec, n = 5). Any presence of apnea was recorded, and animals were hemodynamically stabilized if necessary. Sham animals were induced, attached to the HYGE device without firing it, and were kept under anesthesia for the same amount of time as injured animals (n = 8).

*Laminar Multichannel In Vivo Neurophysiological Recordings in Porcine Hippocampus*: Prior to electrode insertion, pigs undergoing electrophysiological recordings (sham: n = 8 animals; post-TBI: n = 9 animals) were placed in a stereotaxic frame as previously described (Ulyanova, Koch et al. 2018). Large animal stereotaxis combined with single-unit electrophysiological mapping was used to precisely place a 32-channel laminar silicon probe into the CA1 region of the dorsal hippocampus. Laminar oscillatory field potentials and single-unit activity was recorded concurrently in the dorsal hippocampus of pigs under anesthesia. For lamina multichannel recordings, either a NN32/LIN linear 32-channel silicon probe (100 μm or 300 μm spacing between individual channels, Cat# P1x32-70mm-100/300-314r-HP32, NeuroNexus) or a NN32/TET custom-design 32-channel silicon probe (275 μm spacing between individual tetrodes, Cat# V1x32-15mm-tet-lin-177, NeuroNexus) was used for electrophysiological recordings (see (Ulyanova, Cottone et al. 2019) for more details on multichannel silicon probes used in this study). In addition, electrical stimulation was performed in the Schaffer Collaterals using custom-designed concentric bipolar electrodes (Cat# CBBPC75(AU1), FHC) to investigate CA1 responses to the inputs coming in from the hippocampal CA3 layer. At the end of the procedure, the level of anesthesia was deepened, and pigs were sacrificed for histological analysis.

*Neural Data Collection and Analysis*: Electrophysiological recordings were performed under isoflurane anesthesia (2 - 2.5 %). Neurophysiological signals were amplified and acquired continuously at 32 kHz on a 64-channel Digital Lynx 4SX acquisition system with Cheetah recording and acquisition software (Neuralynx, Inc.). The final location of

the silicon probes was confirmed electrophysiologically as described previously (Ulyanova, Koch et al. 2018). Briefly, the pyramidal CA1 layer was identified by calculating the root mean squared (RMS) power in the 600 - 6,000 Hz frequency band, a proxy for the spiking activity of neurons. The following analyses were performed:

*Spike Detection and Analysis: Neural* signals acquired from a tungsten monopolar electrode during the mapping procedure were bandpass filtered (600 Hz to 6 kHz) and thresholded for spike detection in real time. Thresholds were chosen based on observed signal to noise ratios during the session. Neural signals acquired from the lamina multichannel silicon probe were bandpass filtered (0.1 Hz to 9 kHz) in real time prior to sampling. Off-line spike detection and sorting was performed on the wideband signals using the Klusta software packages (http://klusta-team.github.io/klustakwik/), and clusters were manually refined with KlustaViewa software (https://github.com/klusta-team/klustaviewa) (Rossant, Kadir et al. 2016). Resulting single-unit clusters were then imported into Matlab software, version R2017a, for visualization and further analysis using custom and built-in routines (https://www.mathworks.com/products/matlab.html). In order to minimize waveform shape distortion for visualization, the wideband signal was high pass filtered using a wavelet multi-level decomposition and reconstruction filter (level 6, Daubechies 4 wavelet) (Wiltschko, Gage et al. 2008). Waveforms were then extracted from this filtered signal and averaged for display. The freely available Matlab packages FMAToolbox (http://fmatoolbox.sourceforge.net (Hazan, Zugaro et al. 2006)) and Chronux (http://chronux.org (Hazan, Zugaro et al. 2006, Mitra 2007)) were used for analysis of neuronal bursting properties.

*Putative Neuron Subtype Classification:* Hippocampal CA1 cells were classified into groups of putative pyramidal cells and inhibitory interneurons (for review, see (Wheeler, White et al. 2015)) following previously described protocols (Csicsvari, Hirase et al. 1999, Broussard, Redell et al. 2020). Briefly, the following criteria were used: 1) only single units from the top portion of the multichannel silicon probe were selected, which anatomically corresponded to the pyramidal CA1 cell layer; 2) the firing rate of pyramidal cells is < 7 Hz, while firing rate of interneurons is > 7 Hz (under anesthesia); 3) firing probability and spike waveforms for putative CA1 pyramidal cells and CA1 interneurons matched previously published criteria (Csicsvari, Hirase et al. 1999, Broussard, Redell et

al. 2020). Specifically, the firing probability defined as the first moment on the autocorrelogram and the symmetry of the action potential waveform were considered according to the previously described methodology (Csicsvari, Hirase et al. 1999).

*Analysis of Local Field Potentials (LFP):* Acquired wideband LFPs recorded with the 32-channel silicon probe were downsampled to 2 kHz for further analysis. Signals were imported into Matlab software, version R2017a and processed using a combination of custom and modified routines from the freely available Matlab packages FMAToolbox (http://fmatoolbox.sourceforge.net (Hazan, Zugaro et al. 2006)), Chronux (http://chronux.org (Hazan, Zugaro et al. 2006, Mitra 2007)), EEGLAB (http://sccn.ucsd.edu/eeglab/index.html (Delorme and Makeig 2004)), and CSDplotter, version 0.1.1 (Pettersen, Devor et al. 2006).

*Entrainment Analysis:* Entrainment strength was determined by computing the modulation vector length (MVL) each single unit with oscillations ranging from 1 – 300 Hz on the channel that contained the maximal spike amplitude. Entrainment strength for all single units was then averaged and compared between the sham and post-mTBI groups.

*Power Spectrum Density (PSD):* PSD analysis of hippocampal oscillations was performed for all channels with detectable single units. If more than one single unit was recorded on the same channel, the duplicate power spectrum was excluded from the analysis. The calculated PSD was averaged across all animals, then z-score normalized for comparative analysis between the sham and post-mTBI groups of animals.

*NEURON Modeling*: The NEURON simulation environment was used to model the concussion-associated electrophysiological changes observed in CA1 interneurons (Hines and Carnevale 1997, Hines and Carnevale 2001). Specifically, a model of parvalbumin-positive ($PV^+$) basket cells, fast-spiking CA1 interneurons that synapse on the somata and proximal dendrites of CA1 pyramidal cells, was used as described previously (Migliore, Hoffman et al. 1999, Bezaire, Raikov et al. 2016). The individual parameters of the model (activation / inactivation and the maximum conductance of voltage gated channels, ionic driving force, action potential amplitude, number of dendrites per neuron, etc.) were altered either alone or in a combination with other

parameters in a blinded manner to fit the experimental data (summarized in Table 1). The action potentials of the model-generated interneurons were generated and then compared to the experimentally observed values of the firing rate, spike amplitude and spike width following concussion. The parameter(s) most likely to be affected by the injury were identified based on the best fit between experimentally observed data and the NEURON model generated values.

*Statistical Analyses:* The data were analyzed using Matlab (version R2017a, custom and built-in routines) as well as Graphpad Prism (version 7) software. Unpaired t-test was used for comparative analysis between the sham and post-mTBI groups of animals. Ordinary one-way ANOVA was used for comparative analysis between the sham, ~190 rad/sec, and ~260 rad/sec groups of animals. Threshold for significance was used with p-value of less than 0.05. All data presented as mean ± SEM unless otherwise indicated.

## References


Agrawal, A., J. Timothy, L. Pandit and M. Manju (2006). "Post-traumatic epilepsy: An overview." Clinical Neurology and Neurosurgery **108**(5): 433-439. DOI: https://doi.org/10.1016/j.clineuro.2005.09.001

Amit, K., B.-B. Odeya, R. Guy, G. Tal, S. Moatasim, S. Yigal and B. Mony (2017). "Posttraumatic epilepsy: long-term follow-up of children with mild traumatic brain injury." Journal of Neurosurgery: Pediatrics PED **20**(1): 64-70. DOI: https://doi.org/10.3171/2017.2.PEDS16585

Anita, S., T.-S. Lori and R. W. Kathryn (2008). "Prolonged recovery of memory functioning after mild traumatic brain injury in adolescent athletes." Journal of Neurosurgery JNS **108**(3): 511-516. DOI: https://doi.org/10.3171/JNS/2008/108/3/0511

Bazarian, J. J., J. McClung, M. N. Shah, Y. Ting Cheng, W. Flesher and J. Kraus (2005). "Mild traumatic brain injury in the United States, 1998–2000." Brain Injury **19**(2): 85-91. DOI: https://doi.org/10.1080/02699050410001720158

Bezaire, M. J., I. Raikov, K. Burk, D. Vyas and I. Soltesz (2016). "Interneuronal mechanisms of hippocampal theta oscillations in a full-scale model of the rodent CA1 circuit." eLife **5**: e18566. DOI: https://doi.org/10.7554/eLife.18566

Boucher, P.-A., B. Joós and C. E. Morris (2012). "Coupled left-shift of Nav channels: modeling the Na+-loading and dysfunctional excitability of damaged axons." Journal of Computational Neuroscience **33**(2): 301-319. DOI: https://doi.org/10.1007/s10827-012-0387-7

Bragin, A., L. Li, J. Almajano, C. Alvarado-Rojas, A. Y. Reid, R. J. Staba and J. Engel Jr (2016). "Pathologic electrographic changes after experimental traumatic brain injury." Epilepsia **57**(5): 735-745. DOI: https://doi.org/10.1111/epi.13359

Broussard, J. I., J. B. Redell, J. Zhao, M. E. Maynard, N. Kobori, A. Perez, K. N. Hood, X. O. Zhang, A. N. Moore and P. K. Dash (2020). "Mild Traumatic Brain Injury Decreases Spatial Information Content and Reduces Place Field Stability of Hippocampal CA1 Neurons." Journal of neurotrauma **37**(2): 227-235. DOI: https://www.ncbi.nlm.nih.gov/pubmed/31530217

Buzsáki, G. and X.-J. Wang (2012). "Mechanisms of Gamma Oscillations." Annual Review of Neuroscience **35**(1): 203-225. DOI: https://doi.org/10.1146/annurev-neuro-062111-150444

Carr, M. F., S. P. Jadhav and L. M. Frank (2011). "Hippocampal replay in the awake state: a potential substrate for memory consolidation and retrieval." Nature neuroscience **14**(2): 147-153. DOI: https://doi.org/10.1038/nn.2732

Carron, S. F., M. Sun, S. R. Shultz and R. Rajan (2020). "Inhibitory neuronal changes following a mixed diffuse-focal model of traumatic brain injury." Journal of Comparative Neurology **528**(2): 175-198. DOI: https://doi.org/10.1002/cne.24746

Catterall, W. A. (2018). "Dravet Syndrome: A Sodium Channel Interneuronopathy." Current opinion in physiology **2**: 42-50. DOI: https://doi.org/10.1016/j.cophys.2017.12.007

Colgin, L. L. and E. I. Moser (2010). "Gamma Oscillations in the Hippocampus." Physiology **25**(5): 319-329. DOI: https://doi.org/10.1152/physiol.00021.2010

Coronado, V. G., L. C. McGuire, K. Sarmiento, J. Bell, M. R. Lionbarger, C. D. Jones, A. I. Geller, N. Khoury and L. Xu (2012). "Trends in Traumatic Brain Injury in the U.S. and the public health response: 1995–2009." Journal of Safety Research **43**(4): 299-307. DOI: https://doi.org/10.1016/j.jsr.2012.08.011

Csicsvari, J., H. Hirase, A. Czurkó, A. Mamiya and G. Buzsáki (1999). "Oscillatory Coupling of Hippocampal Pyramidal Cells and Interneurons in the Behaving Rat." The Journal of Neuroscience **19**(1): 274. DOI: http://www.jneurosci.org/content/19/1/274.abstract

Cullen, D. K., J. P. Harris, K. D. Browne, J. A. Wolf, J. E. Duda, D. F. Meaney, S. S. Margulies and D. H. Smith (2016). A Porcine Model of Traumatic Brain Injury via Head Rotational Acceleration. Injury Models of the Central Nervous System: Methods and Protocols. F. H. Kobeissy, C. E. Dixon, R. L. Hayes and S. Mondello. New York, NY, Springer New York**:** 289-324. DOI: http://dx.doi.org/10.1007/978-1-4939-3816-2_17

de Almeida Licurgo, I. M., Lisman John E (2009). "A Second Function of Gamma Frequency Oscillations: An E%-Max Winner-Take-All Mechanism Selects Which Cells Fire." The Journal of Neuroscience **29**(23): 7497–7503. DOI: https://doi.org/10.1523/JNEUROSCI.6044-08.2009

de Freitas Cardoso, M. G., R. M. Faleiro, J. J. de Paula, A. Kummer, P. Caramelli, A. L. Teixeira, L. C. de Souza and A. S. Miranda (2019). "Cognitive Impairment Following Acute Mild Traumatic Brain Injury." Frontiers in Neurology **10**: 198. DOI: https://doi.org/10.3389/fneur.2019.00198

Delorme, A. and S. Makeig (2004). "EEGLAB: an open source toolbox for analysis of single-trial EEG dynamics including independent component analysis." Journal of Neuroscience Methods **134**(1): 9-21. DOI: https://doi.org/10.1016/j.jneumeth.2003.10.009

Eijkelkamp, N., J. E. Linley, M. D. Baker, M. S. Minett, R. Cregg, R. Werdehausen, F. Rugiero and J. N. Wood (2012). "Neurological perspectives on voltage-gated sodium channels." Brain **135**(9): 2585-2612. DOI: https://doi.org/10.1093/brain/aws225

Figueiredo, T., C. L. Harbert, V. Pidoplichko, C. P. Almeida-Suhett, K. Rossetti, M. F. M. Braga and A. M. Marini (2020). "The Recovery of GABAergic Function in the Hippocampus CA1 Region After mTBI." Molecular Neurobiology **57**(1): 23-31. DOI: https://doi.org/10.1007/s12035-019-01753-z

Giza, C., T. Greco and M. L. Prins (2018). Chapter 6 - Concussion: pathophysiology and clinical translation. Handbook of Clinical Neurology. B. Hainline and R. A. Stern, Elsevier. **158:** 51-61. DOI: https://doi.org/10.1016/B978-0-444-63954-7.00006-9

Gloveli, T., T. Dugladze, S. Saha, H. Monyer, U. Heinemann, R. D. Traub, M. A. Whittington and E. H. Buhl (2005). "Differential involvement of oriens/pyramidale interneurones in hippocampal network oscillations in vitro." The Journal of physiology **562**(Pt 1): 131-147. DOI: https://doi.org/10.1113/jphysiol.2004.073007

Gold, C., D. A. Henze, C. Koch and G. Buzsáki (2006). "On the Origin of the Extracellular Action Potential Waveform: A Modeling Study." Journal of Neurophysiology **95**(5): 3113-3128. DOI: https://doi.org/10.1152/jn.00979.2005
Grovola, M. R., N. Paleologos, D. P. Brown, N. Tran, K. L. Wofford, J. P. Harris, K. D. Browne, P. A. Shewokis, J. A. Wolf, D. K. Cullen and J. E. Duda (2021). "Diverse changes in microglia morphology and axonal pathology during the course of 1 year after mild traumatic brain injury in pigs." Brain pathology. **31**(5). DOI: https://doi.org/10.1111/bpa.12953
Hazan, L., M. Zugaro and G. Buzsáki (2006). "Klusters, NeuroScope, NDManager: A free software suite for neurophysiological data processing and visualization." Journal of Neuroscience Methods **155**(2): 207-216. DOI: https://doi.org/10.1016/j.jneumeth.2006.01.017
Helmick, K. M., C. A. Spells, S. Z. Malik, C. A. Davies, D. W. Marion and S. R. Hinds (2015). "Traumatic brain injury in the US military: epidemiology and key clinical and research programs." Brain Imaging and Behavior **9**(3): 358-366. DOI: https://doi.org/10.1007/s11682-015-9399-z
Hines, M. L. and N. T. Carnevale (1997). "The NEURON Simulation Environment." Neural Computation **9**(6): 1179-1209. DOI: https://doi.org/10.1162/neco.1997.9.6.1179
Hines, M. L. and N. T. Carnevale (2001). "Neuron: A Tool for Neuroscientists." The Neuroscientist **7**(2): 123-135. DOI: https://doi.org/10.1177/107385840100700207
Hotka, M. and H. Kubista (2019). "The paroxysmal depolarization shift in epilepsy research." The International Journal of Biochemistry & Cell Biology **107**: 77-81. DOI: https://doi.org/10.1016/j.biocel.2018.12.006
Hunt, R. F., S. W. Scheff and B. N. Smith (2011). "Synaptic reorganization of inhibitory hilar interneuron circuitry after traumatic brain injury in mice." The Journal of neuroscience : the official journal of the Society for Neuroscience **31**(18): 6880-6890. DOI: https://doi.org/10.1523/JNEUROSCI.0032-11.2011
Huusko, N., C. Römer, X. E. Ndode-Ekane, K. Lukasiuk and A. Pitkänen (2015). "Loss of hippocampal interneurons and epileptogenesis: a comparison of two animal models of acquired epilepsy." Brain structure & function **220**(1): 153-191. DOI: https://doi.org/10.1007/s00429-013-0644-1
Iwata, A., P. K. Stys, J. A. Wolf, X.-H. Chen, A. G. Taylor, D. F. Meaney and D. H. Smith (2004). "Traumatic axonal injury induces proteolytic cleavage of the voltage-gated sodium channels modulated by tetrodotoxin and protease inhibitors." The Journal of neuroscience : the official journal of the Society for Neuroscience **24**(19): 4605-4613. DOI: https://doi.org/10.1523/JNEUROSCI.0515-03.2004
Johnson, V. E., W. Stewart, M. T. Weber, D. K. Cullen, R. Siman and D. H. Smith (2016). "SNTF immunostaining reveals previously undetected axonal pathology in traumatic brain injury." Acta Neuropathologica **131**(1): 115-135. DOI: https://doi.org/10.1007/s00401-015-1506-0
Johnson, V. E., M. T. Weber, R. Xiao, D. K. Cullen, D. F. Meaney, W. Stewart and D. H. Smith (2018). "Mechanical disruption of the blood-brain barrier following experimental concussion." Acta neuropathologica **135**(5): 711-726. DOI: https://doi.org/10.1007/s00401-018-1824-0
King, N. S. and S. Kirwilliam (2011). "Permanent post-concussion symptoms after mild head injury." Brain Injury **25**(5): 462-470. DOI: https://doi.org/10.3109/02699052.2011.558042
King, R., A. Kirton, E. Zewdie, T. A. Seeger, P. Ciechanski and K. M. Barlow (2019). "Longitudinal Assessment of Cortical Excitability in Children and Adolescents With Mild Traumatic Brain Injury and Persistent Post-concussive Symptoms." Frontiers in Neurology **10**: 451. DOI: https://doi.org/10.3389/fneur.2019.00451
Klausberger, T. and P. Somogyi (2008). "Neuronal Diversity and Temporal Dynamics: The Unity of Hippocampal Circuit Operations." Science **321**(5885): 53. DOI: https://doi.org/10.1126/science.1149381
Koch, H., S.-E. Huh, F. P. Elsen, M. S. Carroll, R. D. Hodge, F. Bedogni, M. S. Turner, R. F. Hevner and J.-M. Ramirez (2010). "Prostaglandin E2-Induced Synaptic Plasticity in Neocortical

Networks of Organotypic Slice Cultures." The Journal of Neuroscience **30**(35): 11678. DOI: https://doi.org/10.1523/JNEUROSCI.4665-09.2010
Koch, P. F., C. Cottone, C. D. Adam, A. V. Ulyanova, R. J. Russo, M. T. Weber, J. D. Arena, V. E. Johnson and J. A. Wolf (2020). "Traumatic Brain Injury Preserves Firing Rates but Disrupts Laminar Oscillatory Coupling and Neuronal Entrainment in Hippocampal CA1." eneuro: ENEURO.0495-0419.2020. DOI: https://doi.org/10.1523/ENEURO.0495-19.2020
Langer, L., C. Levy and M. Bayley (2020). "Increasing Incidence of Concussion: True Epidemic or Better Recognition?" The Journal of Head Trauma Rehabilitation **35**(1). DOI: https://doi.org/10.1097/HTR.0000000000000503
Levin, H. S., N. R. Temkin, J. Barber, L. D. Nelson, C. Robertson, J. Brennan, M. B. Stein, J. K. Yue, J. T. Giacino, M. A. McCrea, R. Diaz-Arrastia, P. Mukherjee, D. O. Okonkwo, K. Boase, A. J. Markowitz, Y. Bodien, S. Taylor, M. J. Vassar, G. T. Manley and T.-T. Investigators (2021). "Association of Sex and Age With Mild Traumatic Brain Injury–Related Symptoms: A TRACK-TBI Study." JAMA Network Open **4**(4): e213046-e213046. DOI: https://doi.org/10.1001/jamanetworkopen.2021.3046
Liautard, C., P. Scalmani, G. Carriero, M. Curtis, S. Franceschetti and M. Mantegazza (2013). "Hippocampal hyperexcitability and specific epileptiform activity in a mouse model of Dravet syndrome." Epilepsia **54**(7): 1251-1261. DOI: https://doi.org/10.1111/epi.12213
Lolk, K., J. W. Dreier and J. Christensen (2021). "Repeated traumatic brain injury and risk of epilepsy: a Danish nationwide cohort study." Brain. DOI: https://doi.org/10.1093/brain/awaa448
Lustig, B., Y. Wang and E. Pastalkova (2015). "Oscillatory patterns in hippocampus under light and deep isoflurane anesthesia closely mirror prominent brain states in awake animals." Hippocampus **26**(1): 102-109. DOI: https://doi.org/10.1002/hipo.22494
MacMullin, P., N. Hodgson, U. Damar, H. H. C. Lee, M. Q. Hameed, S. C. Dhamne, D. Hyde, G. M. Conley, N. Morriss, J. Qiu, R. Mannix, T. K. Hensch and A. Rotenberg (2020). "Increase in Seizure Susceptibility After Repetitive Concussion Results from Oxidative Stress, Parvalbumin-Positive Interneuron Dysfunction and Biphasic Increases in Glutamate/GABA Ratio." Cerebral Cortex **30**(12): 6108-6120. DOI: https://doi.org/10.1093/cercor/bhaa157
Major, B. P., M. A. Rogers and A. J. Pearce (2015). "Using transcranial magnetic stimulation to quantify electrophysiological changes following concussive brain injury: A systematic review." Clinical and Experimental Pharmacology and Physiology **42**(4): 394-405. DOI: https://doi.org/10.1111/1440-1681.12363
Mann, E. O., N. Suckling Jm Fau - Hajos, S. A. Hajos N Fau - Greenfield, O. Greenfield Sa Fau - Paulsen and O. Paulsen (2005). "Perisomatic feedback inhibition underlies cholinergically induced fast network oscillations in the rat hippocampus in vitro." Neuron **45**(1): 105-117. DOI: https://doi.org/10.1016/j.neuron.2004.12.016
Mantegazza, M., G. Curia, G. Biagini, D. S. Ragsdale and M. Avoli (2010). "Voltage-gated sodium channels as therapeutic targets in epilepsy and other neurological disorders." The Lancet Neurology **9**(4): 413-424. DOI: https://doi.org/10.1016/S1474-4422(10)70059-4
Migliore, M., D. A. Hoffman, J. C. Magee and D. Johnston (1999). "Role of an A-type K+ conductance in the back-propagation of action potentials in the dendrites of hippocampal pyramidal neurons." Journal of computational neuroscience **7**(1): 5-15. DOI: https://doi.org/10.1023/a:1008906225285
Mitra, P. P. B., Hemant (2007). Observed brain dynamics, Oxford University Press.
Munyon, C., K. C. Eakin, J. A. Sweet and J. P. Miller (2014). "Decreased bursting and novel object-specific cell firing in the hippocampus after mild traumatic brain injury." Brain research **1582**: 220-226. DOI: https://doi.org/10.1016/j.brainres.2014.07.036
Nichols, J., G. R. Bjorklund, J. Newbern and T. Anderson (2018). "Parvalbumin fast-spiking interneurons are selectively altered by paediatric traumatic brain injury." The Journal of Physiology **596**(7): 1277-1293. DOI: https://doi.org/10.1113/JP275393

Ogiwara, I., H. Miyamoto, N. Morita, N. Atapour, E. Mazaki, I. Inoue, T. Takeuchi, S. Itohara, Y. Yanagawa, K. Obata, T. Furuichi, T. K. Hensch and K. Yamakawa (2007). "Nav1.1 localizes to axons of parvalbumin-positive inhibitory interneurons: a circuit basis for epileptic seizures in mice carrying an Scn1a gene mutation." The Journal of neuroscience : the official journal of the Society for Neuroscience **27**(22): 5903-5914. DOI: https://doi.org/10.1523/JNEUROSCI.5270-06.2007

Ondek, K., A. Pevzner, K. Tercovich, A. M. Schedlbauer, A. Izadi, A. D. Ekstrom, S. L. Cowen, K. Shahlaie and G. G. Gurkoff (2020). "Recovery of Theta Frequency Oscillations in Rats Following Lateral Fluid Percussion Corresponds With a Mild Cognitive Phenotype." Frontiers in Neurology **11**. DOI: https://doi.org/10.3389/fneur.2020.600171

Paterno, R., H. Metheny, G. Xiong, J. Elkind and A. S. Cohen (2015). "Mild Traumatic Brain Injury Decreases Broadband Power in Area CA1." Journal of Neurotrauma **33**(17): 1645-1649. DOI: https://doi.org/10.1089/neu.2015.4107

Pavlov, I., A. Scimemi, L. Savtchenko, D. M. Kullmann and M. C. Walker (2011). "Ih-mediated depolarization enhances the temporal precision of neuronal integration." Nature Communications **2**(1): 199. DOI: https://doi.org/10.1038/ncomms1202

Pelkey, K. A., R. Chittajallu, M. T. Craig, L. Tricoire, J. C. Wester and C. J. McBain (2017). "Hippocampal GABAergic Inhibitory Interneurons." Physiological Reviews **97**(4): 1619-1747. DOI: https://doi.org/10.1152/physrev.00007.2017

Pettersen, K. H., A. Devor, I. Ulbert, A. M. Dale and G. T. Einevoll (2006). "Current-source density estimation based on inversion of electrostatic forward solution: effects of finite extent of neuronal activity and conductivity discontinuities." Journal of neuroscience methods **154**(1-2): 116-133. DOI: https://doi.org/10.1016/j.jneumeth.2005.12.005

Pike, F. G., R. S. Goddard, J. M. Suckling, P. Ganter, N. Kasthuri and O. Paulsen (2000). "Distinct frequency preferences of different types of rat hippocampal neurones in response to oscillatory input currents." The Journal of physiology **529 Pt 1**(Pt 1): 205-213. DOI: https://doi.org/10.1111/j.1469-7793.2000.00205.x

Rabinowitz, A. R., X. Li, S. R. McCauley, E. A. Wilde, A. Barnes, G. Hanten, D. Mendez, J. J. McCarthy and H. S. Levin (2015). "Prevalence and Predictors of Poor Recovery from Mild Traumatic Brain Injury." Journal of Neurotrauma **32**(19): 1488-1496. DOI: https://doi.org/10.1089/neu.2014.3555

Rennó-Costa, C., D. G. Teixeira and I. Soltesz (2019). "Regulation of gamma-frequency oscillation by feedforward inhibition: A computational modeling study." Hippocampus **29**(10): 957-970. DOI: https://doi.org/10.1002/hipo.23093

Røe, C., U. Sveen, K. Alvsåker and E. Bautz-Holter (2009). "Post-concussion symptoms after mild traumatic brain injury: influence of demographic factors and injury severity in a 1-year cohort study." Disability and Rehabilitation **31**(15): 1235-1243. DOI: https://doi.org/10.1080/09638280802532720

Rossant, C., S. N. Kadir, D. F. M. Goodman, J. Schulman, M. L. D. Hunter, A. B. Saleem, A. Grosmark, M. Belluscio, G. H. Denfield, A. S. Ecker, A. S. Tolias, S. Solomon, G. Buzsaki, M. Carandini and K. D. Harris (2016). "Spike sorting for large, dense electrode arrays." Nat Neurosci **19**(4): 634-641. DOI: http://dx.doi.org/10.1038/nn.4268

Schmitt, S. and M. A. Dichter (2015). Chapter 21 - Electrophysiologic recordings in traumatic brain injury. Handbook of Clinical Neurology. J. Grafman and A. M. Salazar, Elsevier. **127:** 319-339. DOI: https://doi.org/10.1016/B978-0-444-52892-6.00021-0

Sengupta, B., A. A. Faisal, S. B. Laughlin and J. E. Niven (2013). "The effect of cell size and channel density on neuronal information encoding and energy efficiency." Journal of cerebral blood flow and metabolism : official journal of the International Society of Cerebral Blood Flow and Metabolism **33**(9): 1465-1473. DOI: https://doi.org/10.1038/jcbfm.2013.103

Singh, R., T. B. Meier, R. Kuplicki, J. Savitz, I. Mukai, L. Cavanagh, T. Allen, T. K. Teague, C. Nerio, D. Polanski and P. S. F. Bellgowan (2014). "Relationship of Collegiate Football Experience

and Concussion With Hippocampal Volume and Cognitive Outcomes." JAMA **311**(18): 1883-1888. DOI: https://doi.org/10.1001/jama.2014.3313
Soltesz, I. and M. Deschênes (1993). "Low- and high-frequency membrane potential oscillations during theta activity in CA1 and CA3 pyramidal neurons of the rat hippocampus under ketamine-xylazine anesthesia". Journal of Neurophysiology **70**(1) Pages 97-116. DOI: https://doi.org/10.1152/jn.1993.70.1.97
J. Spampanato, J. A. Kearney, G. de Haan, D. P. McEwen, A. Escayg, I. Aradi, B. T. MacDonald, S. I. Levin, I. Soltesz, P. Benna, E. Montalenti, L. L. Isom, A. L. Goldin and M. H. Meisler (2004). "A Novel Epilepsy Mutation in the Sodium Channel SCN1A Identifies a Cytoplasmic Domain for β Subunit Interaction". Journal of Neuroscience **24**(44): 10022-10034; DOI: https://doi.org/10.1523/JNEUROSCI.2034-04.2004
Sterr, A., K. A. Herron, C. Hayward and D. Montaldi (2006). "Are mild head injuries as mild as we think? Neurobehavioral concomitants of chronic post-concussion syndrome." BMC Neurology **6**(1): 7. DOI: https://doi.org/10.1186/1471-2377-6-7
Strain, J. F., K. B. Womack, N. Didehbani, J. S. Spence, H. Conover, J. Hart, Jr., M. A. Kraut and C. M. Cullum (2015). "Imaging Correlates of Memory and Concussion History in Retired National Football League Athletes." JAMA Neurology **72**(7): 773-780. DOI: https://doi.org/10.1001/jamaneurol.2015.0206
Thompson, S. A., B. Krishnan, J. Gonzalez-Martinez, J. Bulacio, L. Jehi, J. Mosher, A. Alexopoulos and R. C. Burgess (2016). "Ictal infraslow activity in stereoelectroencephalography: Beyond the “DC shift”." Clinical Neurophysiology **127**(1): 117-128.
Thompson, S. A., B. Krishnan, J. Gonzalez-Martinez, J. Bulacio, L. Jehi, J. Mosher, A. Alexopoulos and R. C. Burgess (2016). "Interictal Infraslow Activity in Stereoelectroencephalography: From Focus to Network." Journal of Clinical Neurophysiology **33**(2).
Toth, Z., G. S. Hollrigel, T. Gorcs and I. Soltesz (1997). "Instantaneous perturbation of dentate interneuronal networks by a pressure wave-transient delivered to the neocortex." The Journal of neuroscience : the official journal of the Society for Neuroscience **17**(21): 8106-8117. DOI: https://doi.org/10.1523/JNEUROSCI.17-21-08106.1997
Ulyanova, A. V., C. Cottone, C. D. Adam, K. G. Gagnon, D. K. Cullen, T. Holtzman, B. G. Jamieson, P. F. Koch, H. I. Chen, V. E. Johnson and J. A. Wolf (2019). "Multichannel Silicon Probes for Awake Hippocampal Recordings in Large Animals." Frontiers in Neuroscience **13**: 397. DOI: https://doi.org/10.3389/fnins.2019.00397
Ulyanova, A. V., P. F. Koch, C. Cottone, M. R. Grovola, C. D. Adam, K. D. Browne, M. T. Weber, R. J. Russo, K. G. Gagnon, D. H. Smith, H. Isaac Chen, V. E. Johnson, D. Kacy Cullen and J. A. Wolf (2018). "Electrophysiological Signature Reveals Laminar Structure of the Porcine Hippocampus." eNeuro **5**(5): ENEURO.0102-0118.2018. DOI: https://doi.org/10.1523/ENEURO.0102-18.2018
Veliz, P., S. E. McCabe, J. T. Eckner and J. E. Schulenberg (2021). "Concussion, sensation-seeking and substance use among US adolescents." Substance Abuse **42**(2): 183-191. DOI: https://doi.org/10.1080/08897077.2019.1671938
Vilin, Y. Y. and P. C. Ruben (2001). "Slow inactivation in voltage-gated sodium channels: molecular substrates and contributions to channelopathies." Cell Biochemistry and Biophysics **35**(2): 171-190. DOI: https://doi.org/10.1385/CBB:35:2:171
Wheeler, D. W., C. M. White, C. L. Rees, A. O. Komendantov, D. J. Hamilton and G. A. Ascoli (2015). "Hippocampome.org: a knowledge base of neuron types in the rodent hippocampus." eLife **4**: e09960. DOI: https://doi.org/10.7554/eLife.09960
Wiltschko, A. B., G. J. Gage and J. D. Berke (2008). "Wavelet filtering before spike detection preserves waveform shape and enhances single-unit discrimination." Journal of Neuroscience Methods **173**(1): 34-40. DOI: DOI: http://dx.doi.org/10.1016/j.jneumeth.2008.05.016

Witgen, B. M., J. Lifshitz, M. L. Smith, E. Schwarzbach, S. L. Liang, M. S. Grady and A. S. Cohen (2005). "Regional hippocampal alteration associated with cognitive deficit following experimental brain injury: A systems, network and cellular evaluation." Neuroscience **133**(1): 1-15. DOI: https://doi.org/10.1016/j.neuroscience.2005.01.052

Wofford, K. L., M. R. Grovola, D. O. Adewole, K. D. Browne, M. E. Putt, J. C. O'Donnell and D. K. Cullen (2021). "Relationships between injury kinematics, neurological recovery, and pathology following concussion." Brain communications **3**(4): fcab268-fcab268. DOI: https://doi.org/10.1093/braincomms/fcab268

Wolf, J. A., B. N. Johnson, V. E. Johnson, M. E. Putt, K. D. Browne, C. J. Mietus, D. P. Brown, K. L. Wofford, D. H. Smith, M. S. Grady, A. S. Cohen and D. K. Cullen (2017). "Concussion Induces Hippocampal Circuitry Disruption in Swine." Journal of Neurotrauma **34**(14): 2303-2314. DOI: https://doi.org/10.1089/neu.2016.4848

Wolf, J. A. and P. F. Koch (2016). "Disruption of Network Synchrony and Cognitive Dysfunction After Traumatic Brain Injury." Frontiers in Systems Neuroscience **10**: 43. DOI: https://doi.org/10.3389/fnsys.2016.00043

Wolf, J. A., P. K. Stys, T. Lusardi, D. Meaney and D. H. Smith (2001). "Traumatic axonal injury induces calcium influx modulated by tetrodotoxin-sensitive sodium channels." The Journal of neuroscience : the official journal of the Society for Neuroscience **21**(6): 1923-1930. DOI: https://doi.org/10.1523/JNEUROSCI.21-06-01923.2001

Yu, F. H., M. Mantegazza, R. E. Westenbroek, C. A. Robbins, F. Kalume, K. A. Burton, W. J. Spain, G. S. McKnight, T. Scheuer and W. A. Catterall (2006). "Reduced sodium current in GABAergic interneurons in a mouse model of severe myoclonic epilepsy in infancy." Nature neuroscience **9**(9): 1142-1149. DOI: https://doi.org/10.1038/nn1754